Progress In Electromagnetics Research C, Vol. 2, 207–215, 2008

FORWARD SCATTERING FROM A FINITE, CIRCULAR CYLINDER

R. A. Ross

MIT Lincoln Laboratory
244 Wood Street, Lexington, MA 02420, USA

Abstract—Forward scattering from a finite, right-circular cylinder is analyzed as a function of size. Both axial and broadside incidence are treated. Predictions based upon combinations of Physical Optics, Wu's series, and empirical formulas are compared with numerical results from the moment method. The analysis examines cylinders that vary between 1 to 20 wavelengths in radius and 0 to 20 wavelengths in length. Approximate formulas accurately model the RCS of cylinders as small as one wavelength in radius. Accuracy of predictions improves with increase in cylinder size.

1. INTRODUCTION

The exact solution for scattering from an infinitely long, perfectly conducting, right-circular cylinder viewed at broadside incidence is attributed to Lord Rayleigh [1]. It has received the most intensive study of all two-dimensional structures [2], and several books contain calculations of bistatic RCS. Ruck et al. [3] present a summary of cylinder studies that includes plots of the bistatic RCS for several radii. Although these bistatic data include the relevant forward scattering case, a cylinder of finite length scatters differently.

The topic of interest, the conventional bistatic RCS in the forward direction, will be called "Forward RCS" and denoted by σ^F. Crispin and Siegel [4] state that the Physical Optics (PO) result for σ^F depends upon the projected area of the object. In the limit of vanishing wavelength, σ^F is the same for all objects having the same projected area, regardless of the shape of the object or the choice of incident polarization. Siegel's [5] claim seems bold in its disregard for scattering parameters as important as shape and polarization. However, it will be shown that PO provides the leading term in σ^F for a finite, right-circular cylinder viewed at axial or broadside incidence.

Forward RCS σ^F is distinct from Total RCS σ^T (sometimes called the Extinction RCS) predicted by the Forward Scattering Theorem (FST) [3]. King and Wu [6] use the FST to predict σ^T for a circular cylinder at practical wavelengths. The perfectly conducting cylinder is infinitely long and illuminated at broadside incidence. Wu expands the solution in an asymptotic series in which the leading term is the Geometric Optics value. The remaining terms depend upon shape though inverse powers of radius. Predictions of σ^T based upon Wu's series agree with computations of the exact eigenfunction expansion for both vertical and horizontal polarization (see Figs. 18 and 19 in [6]).

Siegel's PO result and Wu's series will be included in a formula for the forward RCS of a finite, perfectly-conducting cylinder, which includes two new contributions. Briefly, surfaces that are tangent to the shadow boundary may contribute to forward scattering. At axial incidence, forward scattering depends upon the area of the curved surface of the cylinder. At broadside incidence, forward scattering also depends upon the area of the flat surfaces at the sides. It is these surface area contributions and Wu's series which furnish the shape and polarization information that is missing in PO.

Predictions of σ^F based upon Physical Optics, Wu's series, and empirical formulas are combined in ways guided by results of method of moment (MM) calculations. All quantitative MM data are obtained using the body-of-revolution solution called Cicero [7]. It enables calculation of forward scattering from cylinders between 1 and 20 wavelengths in radius and 0 and 20 wavelengths in length. Much of the data is for cylinders 4 wavelengths long having radii between 2 and 16 wavelengths.

2. ANALYSIS

Figure 1 shows a perfectly conducting, circular cylinder which is symmetrical along the X axis of the coordinate system used for analysis. The cylinder has radius a and length L. *All dimensions are given in wavelengths* where $\lambda = 2.54\,\text{cm}$. Illumination by a plane wave is depicted with its wave propagation vector confined to the X-Y plane, and $e^{-j\varpi t}$ time dependence is suppressed. The incidence angle (α_{Inc}) and observation angle ($\alpha_{Obs} = \alpha_{Inc} + 180^\circ$) are measured from the X-axis and the phase reference is the origin. In Fig. 1, vertical polarization is shown with the electric field vector $\vec{E}$ aligned parallel to the Z-axis: horizontal corresponds to the $\vec{E}$ perpendicular to the Z-axis. The polarization notation is as follows; σ_{vv} denotes vertical polarization RCS, σ_{hh} horizontal, σ_{op} opposite-sense circular, and σ_{pp} same-sense circular.

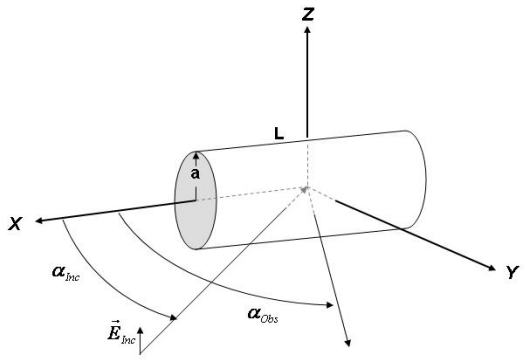

Figure 1. Coordinate system for circular cylinder.

2.1. Axial Incidence

According to Physical Optics, if the wavelength is small, forward RCS depends on the projected area and the phase is purely imaginary [5].

$$\sigma^{PO}(0^\circ) = 4\pi\left(\frac{Area_P}{\lambda}\right)^2 = 4\pi^3\left(\frac{a^2}{\lambda}\right)^2 \text{ and } \rho^{PO}(0^\circ) = \pi/2 \quad (1)$$

where $Area_p$ is the projected area under the curve separating the illuminated and shadowed regions. At axial incidence, the near flat surface and the curved surface are directly illuminated, so the shadow boundary lies at the far end of the cylinder.

The contribution from the curved surface of a cylinder is given empirically by:

$$\sigma^{cs}(0^\circ) = 0.9473 Area_{cs}\left(\frac{H_p}{\lambda}\right) = 3.789(\pi aL)\left(\frac{a}{\lambda}\right) \text{ and } \rho^{cs}(0^\circ) = 3\pi/4 \quad (2)$$

where $Area_{cs} = 2\pi aL$ is the area of the curved surface, and $H_p = 2a$ is the height. Combining (1) and (2), the forward RCS at axial incidence is:

$$\sigma^F_{vv}(0^\circ) = \sigma^F_{hh}(0^\circ) = \left|\sqrt{\sigma^{PO}(0^\circ)}e^{j\pi/2} + \sqrt{\sigma^{cs}(0^\circ)}e^{j3\pi/4}\right|^2 \quad (3)$$

(Symmetry dictates that $\sigma_{vv} = \sigma_{hh} = \sigma_{op}$ and σ_{pp} vanishes.) Fig. 2(a) compares (3) with MM RCS data with $a = 2$, 3 and 4 for $0 \le L \le 16$. For a given radius, the PO RCS for a cylinder and an infinitely thin disk ($L = 0$) are the same. The MM data show a monotonic increase in

RCS with increase in L that is due to currents on the curved surface. By combining terms from PO and the curved surface, (3) provides very accurate estimates of RCS for radii as small as 2.

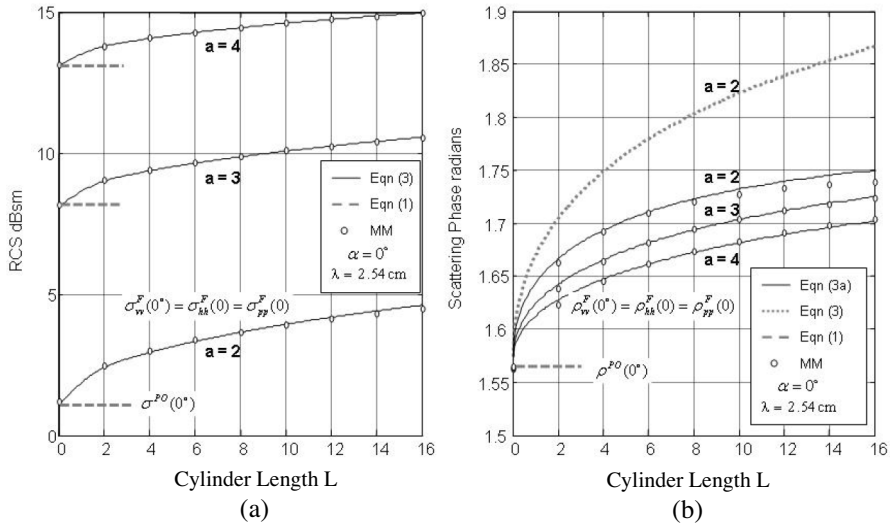

(a) (b)

Figure 2. Forward scattering at axial incidence as function of length. (a) RCS. (b) Phase.

Figure 2(b) shows that the phase for $a = 2$ continues to diverge from MM data as length increases. Although the largest difference is small (~ 0.12 radian), a better approximation is provided for rod-like cylinders viewed axially:

$$\rho_{vv}^{F}(0^\circ) = \rho_{hh}^{F}(0^\circ) = \rho(3) - 0.0656a^{-4/3}L^{0.57} \tag{3a}$$

where $\rho(3)$ denotes the phase predicted by (3). In the region covered by Fig. 2(b), phases now agree to within 0.01 radians.

2.2. Broadside Incidence

At broadside incidence, half of the curved surface ($Y \geq 0$) and the entire flat surfaces are directly illuminated. Forward RCS depends upon polarization in two ways: (1) the curvature of the cylinder at the shadow boundary, and (2) the flat sides. The effect of curvature is explicit in Wu's formulas for the total RCS σ^T of an infinitely long cylinder (17.11) and (17.12) in [6]). To suit the present application,

Wu's asymptotic series is truncated to three terms and the coefficients are reduced to three significant figures:

$$\begin{aligned} W_{hh} &\approx \left[1 + 0.498(ka)^{-2/3} - 0.011(ka)^{-4/3}\right] \\ W_{vv} &\approx \left[1 - 0.432(ka)^{-2/3} - 0.214(ka)^{-4/3}\right] \end{aligned} \tag{4}$$

The first term is the Geometric Optics result, and the terms in inverse powers of (ka) are corrections. The difference in the surface current density near the shadow boundary on the curved surface results in $W_{hh} > W_{vv}$. In order to apply (4), it is first necessary to relate formulas for Forward and Total RCS. Since $\sigma^T \propto Area_p W$, it can be inferred that $\sigma^F \propto Area_p^2 W^2$ so that:

$$\sigma^F(90^\circ) = \sigma^{PO}(90^\circ) W^2 \tag{5}$$

$$\text{where } \sigma^{PO}(90^\circ) = 16\pi \left(\frac{aL}{\lambda}\right)^2 \text{ and } \rho^{PO}(90^\circ) = \pi/2 \tag{5a}$$

In the case of horizontal polarization, W_{hh} increases the PO result:

$$\sigma^F_{hh}(90^\circ) = \sigma^{PO}(90^\circ) W^2_{hh} = 4\pi \left(\frac{2aL}{\lambda} W_{hh}\right)^2 \text{ and } \rho^F_{hh}(90^\circ) = \frac{\pi}{2} \tag{6}$$

Figure 3 quantifies the effect of small curvature on RCS with $4 \leq L \leq 8$. Fig. 3(a) shows that $\sigma^F_{hh}(90^\circ)$ from (6) is in close agreement with MM data whereas σ^{PO} from (5a) underestimates MM RCS by as much as $\sim$1 1/2 dB. For horizontal polarization, PO modified by Wu's series gives an excellent approximation down to $a = 1$.

In the case of vertical polarization, scattering also arises from the flat sides of the finite cylinder. A formula [8] for the contribution from the two sides is:

$$\sigma^{side}_{vv} = \frac{14}{\pi\lambda} Area_S H_p = 28\frac{a^3}{\lambda} \text{ and } \rho^{side}_{vv} = 3\pi/4 \tag{7}$$

where $Area_s = \pi a^2$ is the surface area and $H_p = 2a$ is the height. (Notice that (7) has the same form as (2) with a different constant.) Combining (4), (5) and (7):

$$\sigma^F_{vv}(90^\circ) \approx \left|\sqrt{\sigma^{PO}} W_{vv} e^{j\pi/2} + \sqrt{\sigma^{side}_{vv}} e^{j3\pi/4}\right|^2 \tag{8}$$

RCS data shown in Fig. 3(b) confirm that (8) combines Physical Optics, Wu's series and side contributions properly. Depending upon the choice of radius and length, the RCS (8) may be less than or greater than the PO prediction.

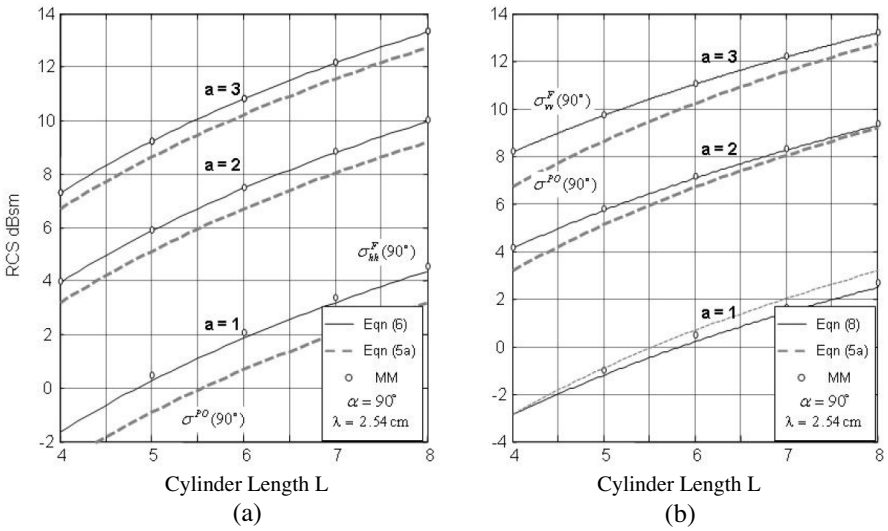

Figure 3. Forward RCS at broadside incidence as function of length. (a) Horizontal polarization. (b) Vertical polarization.

Figure 4 illustrates the effect of large curvature on RCS for a family of cylinders having $L = 4$. In Fig. 4(a), $\sigma^F_{hh}(90°)$ is accurately represented by $\sigma^{PO}(90°)$ because there is no side return and $W_{hh} \approx 1$. On the other hand, $\sigma^F_{vv}(90°)$ becomes as much as 4 dB greater than $\sigma^{PO}(90°)$ largely due to the strong contribution (7) from the flat sides.

Circular polarization RCS is obtained by combining (6) and (8):

$$\sigma^F_{op}(90°) \approx \frac{1}{4}\left|\sqrt{\sigma^F_{hh}(90°)}e^{j\rho_{hh}(90°)} + \sqrt{\sigma^F_{vv}(90°)}e^{j\rho_{vv}(90°)}\right|^2 \quad (9)$$

$$\sigma^F_{pp}(90°) \approx \frac{1}{4}\left|\sqrt{\sigma^F_{hh}(90°)}e^{j\rho_{hh}(90°)} - \sqrt{\sigma^F_{vv}(90°)}e^{j\rho_{vv}(90°)}\right|^2 \quad (10)$$

Figure 4(b) shows RCS results for circular polarization. σ_{pp} is normally greater than σ_{op} in backscattering; the converse is true in forward scattering. $\sigma^F_{op}(90°)$ agrees closely with MM data while $\sigma^F_{pp}(90°)$ falls farther below as the radius increases. $\sigma^F_{pp}(90°)$ is much weaker and close agreement with MM data is not maintained for $a < 6$. Still,

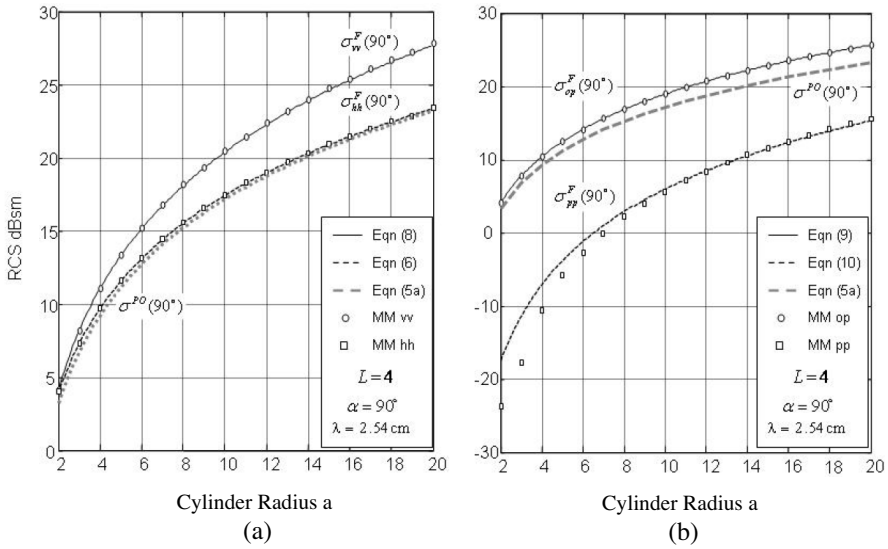

Figure 4. Forward RCS at broadside incidence as function of radius. (a) Linear polarization. (b) Circular polarization.

(10) has value considering the corresponding PO result vanishes for all radii.

Figure 5 compares the corresponding results for scattering phase. The match with MM data for vertical polarization is excellent. Horizontal polarization data agree to within 0.1 radians. The correspondence with opposite-sense circular is also excellent, and same-sense circular RCS matches as well as the horizontal polarization case.

3. DISCUSSION

Forward RCS has been investigated when a finite, right-circular cylinder is illuminated at axial and broadside incidence. Provided a very short cylinder is not viewed broadside, the dominant term is given by PO. A second term, called Wu's series, is due to surface curvature at the shadow boundary. Two new terms, found empirically, are associated with surface areas that are tangent to the shadow boundary. Together, the terms account for the dependence of scattering upon shape and polarization that is observed in MM data.

When all terms are included, predictions are in very close agreement with MM RCS with one exception. Of four polarization combinations examined, only the weakest return (parallel circular

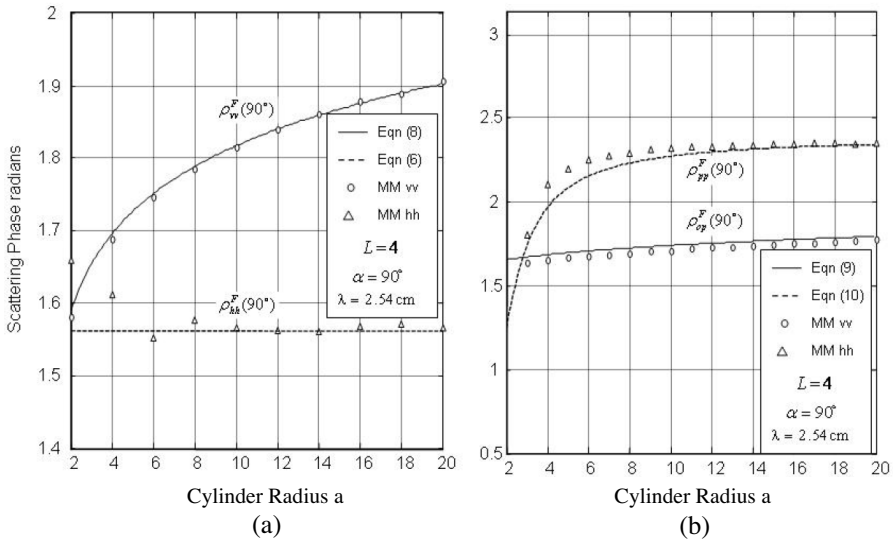

Figure 5. Forward phase at broadside incidence as function of radius. (a) Linear polarization. (b) Circular polarization.

polarization shown in Fig. 4(b)) shows a large mismatch in RCS and only when the radius is not large.

The same approach may be used to predict forward scattering at arbitrary aspects. It remains to determine the aspect dependence of (2) near axial incidence, and (4) and (7) near broadside incidence. This implies that PO given by (1) is adequate at intermediate aspects. Finally, empirical findings about Forward RCS σ^F can be carried over to Total RCS σ^T.

4. CONCLUSIONS

Simple formulas are presented for predicting the forward RCS of a finite, circular cylinder illuminated at axial or broadside incidence. By adding terms to the Physical Optics result, the proper dependence of scattering upon shape and polarization is obtained. RCS estimates are in excellent agreement with moment method calculations when the radius is large, and in most cases when the radius is as small as two wavelengths. The same technique can be used to predict forward scattering at arbitrary incidence angles, and from other objects (e.g., a finite, rectangular cylinder).

ACKNOWLEDGMENT

Mr. Jeremy S. Coombs in Group 34 wrote MATLAB scripts that enable efficient use of the Cicero code in batch mode on a Personal Computer.

This work was sponsored by the Department of the Army under Air Force Contract # FA8721-05-C-0002. Opinions, interpretations, conclusions, and recommendations are those of the author and are not necessarily endorsed by the United States Government.

REFERENCES

1. Strutt, J. W. and L. Rayleigh, "On the electromagnetic theory of light," *Phil. Mag.*, Vol. 12, 81–101, 1881.
2. Bowman, J. J., T. B. A. Senior, and P. L. E. Uslenghi, *Electromagnetic and Acoustic Scattering by Simple Shapes*, Hemisphere Publishing Corp., New York, 1987.
3. Ruck, G. T., D. E. Barrick, W. D. Stuart, and C. K. Kirchbaum, *Radar Cross Section Handbook*, Vol. 1, Plenum Press, New York, 1970.
4. Crispin, Jr., J. W. and K. M. Siegel, *Methods of Radar Cross-section Analysis*, Academic Press, New York, 1968.
5. Siegel, K. M., "Bistatic radars and forward scattering," *Proc. National Conference on Aeronautical Electronics*, 286, Dayton, Ohio, 1958.
6. King, R. W. P. and T. T. Wu, *The Scattering and Diffraction of Waves*, Harvard University Press, Cambridge, 1959.
7. Putnam, J. M. and L. N. Medgyesi-Mitschang, "Combined field integral equation formulation for axially inhomogeneous bodies of revolution," McDonnell Douglas Research Laboratories Technical Report, Vol. 1, No. QA003, 1986.
8. Ross, R. A., "Backscattering from square plates illuminated with vertical polarization," *IEEE Trans. Antennas Propagat.*, Vol. 54, No. 1, 272–275, January 2006.